

# Identification by Isotopic Exchange of Oxygen Deposited on Fe/MFI by Decomposing N<sub>2</sub>O

Jifei Jia, Bin Wen, and Wolfgang M. H. Sachtler<sup>1</sup>

*Institute for Environmental Catalysis, Northwestern University, Evanston, Illinois 60208*

Received April 9, 2002; revised May 28, 2002; accepted May 28, 2002

Isotopic exchange was studied at 250°C between <sup>18</sup>O<sub>2</sub> and Fe/MFI that was prepared by sublimation and subsequently exposed to N<sub>2</sub><sup>16</sup>O. The pretreatment of the Fe/MFI, prior to its contact with N<sub>2</sub>O, is crucial for the kinetics of the subsequent isotopic exchange. Little exchange is observed with materials that were merely reduced at 500°C before dissociative adsorption of N<sub>2</sub>O. However, different adsorption sites are formed by reduction at  $T \geq 600^\circ\text{C}$  or evacuation at 700°C after reduction at 500°C. After such treatment the dissociative adsorption of N<sub>2</sub>O results in a very active oxygen species, identified by rapid isotopic exchange with <sup>18</sup>O<sub>2</sub> at 250°C. The exchange kinetics of these <sup>16</sup>O atoms with <sup>18</sup>O<sub>2</sub> is of the R<sup>1</sup> type, as expected for ferryl oxygen ligated to Fe<sup>4+</sup> ions in Fe/MFI. Only part of the oxygen from N<sub>2</sub>O displays this exchange activity; the number of the rapidly exchanging oxygen atoms is equal, within experimental error, to the number counted by integrating a sharp H<sub>2</sub>-TPR spike at 200°C. Adsorbed water blocks Fe sites for isotopic exchange. © 2002 Elsevier Science (USA)

**Key Words:** active oxygen on Fe/MFI; ferryl groups in zeolite; oxygen isotope exchange; N<sub>2</sub>O dissociation.

## 1. INTRODUCTION

Isotopic exchange between oxygen in the gas phase and a solid oxide is a powerful tool to discriminate between oxygen species of different reactivity (1–6). It is generally accepted that two types of process can be discerned. In one of these, an <sup>18</sup>O<sub>2</sub> molecule contacting a solid containing <sup>16</sup>O atoms will exchange one of its atoms, so that the primary product is an <sup>18</sup>O<sup>16</sup>O molecule. In the second process both atoms are exchanged during one interaction of the molecule with the solid, i.e., <sup>16</sup>O<sub>2</sub> molecules are primary exchange products. If that process prevails, a gas mixture containing the three molecules <sup>16</sup>O<sub>2</sub>, <sup>16</sup>O<sup>18</sup>O, and <sup>18</sup>O<sub>2</sub> initially in equilibrium may temporarily depart from this equilibrium. We follow Klier's nomenclature, calling the former mechanism R<sup>1</sup> and the latter R<sup>2</sup>. In this terminology, an exchange between gaseous <sup>16</sup>O<sub>2</sub> and <sup>18</sup>O<sub>2</sub> without apparent contribution of a solid is conventionally called R<sup>0</sup>.

<sup>1</sup> To whom correspondence should be addressed. Fax: (847) 467-1018. E-mail: wmhs@northwestern.edu.

Previously we reported that Fe/MFI, prepared via sublimation of FeCl<sub>3</sub> on H/MFI, efficiently catalyzes the reduction of the nitrogen oxides NO and NO<sub>2</sub> to N<sub>2</sub> with hydrocarbons (7) or ammonia (8). For these catalysts the formation of oxygen-bridged Fe dimers was proposed and confirmed by XAFS data of Marturano *et al.* (9) and Battiston *et al.* (10). Isotopic exchange between <sup>18</sup>O<sub>2</sub> and such Fe/MFI indicated that the R<sup>1</sup> mechanism is dominant at 400°C but the R<sup>2</sup> mechanism dominates at 450°C (5). Exchange was found to be faster for catalysts containing Fe<sub>2</sub>O<sub>3</sub> clusters than over oxygen-bridged dimers and it included part of the zeolite oxygen atoms of the zeolite in atomic contact with Fe ions. No exchange was observed in the absence of Fe. At higher temperature, N<sub>2</sub>O decomposition over calcined Fe/MFI catalysts was found to display kinetic oscillation in the presence of water vapor (11).

Recently we found that reduction in an H<sub>2</sub> flow at 600°C of Fe/MFI prepared by sublimation, followed by its exposure to N<sub>2</sub>O at 250°C, produced a highly active state characterized by an unusual TPR spike at 200°C (12). *In situ* XANES data, XAFS data, and DFT calculations (13) suggest that in this state some Fe might be present in the oxidation state of Fe<sup>4+</sup>. It is conceivable that the active oxygen in N<sub>2</sub>O-activated Fe/MFI prepared by sublimation is similar to Panov's "α oxygen" that was observed with Fe/MFI of much lower Fe content and prepared by a different method (12). We assume that this active form of oxygen is also similar to that observed by Mauvezin *et al.* after exposing Fe/BEA to N<sub>2</sub>O (14). In this paper we report on <sup>18</sup>O<sub>2</sub> isotope exchange with N<sub>2</sub>O-activated Fe/MFI which has a molar ratio of Fe to Al-centered tetrahedra of 1/1.

## 2. EXPERIMENTAL

### 2.1. Preparation of Fe/MFI

The acidic form of the MFI zeolite, H/MFI, was obtained by three-fold ion exchange Na/MFI (Si/Al = 23, UOP) with a diluted NH<sub>4</sub>NO<sub>3</sub> solution at ambient temperature, followed by calcination of the NH<sub>4</sub><sup>+</sup> form of the zeolite in an ultrahigh purity O<sub>2</sub> flow at 550°C for 4 h. Sublimation of FeCl<sub>3</sub> in flowing Ar at 320°C was used to direct the vapor

onto heated H/MFI, as described in our previous paper (7). After hydrolysis, the slurry was vacuum filtered, the solid was washed thoroughly with DDI (doubly deionized) water, dried at 120°C in air, and calcined in O<sub>2</sub> at 550°C. The Fe/Al ratio is near unity, which corresponds to 4.0 wt% Fe for the dry catalyst. Another Fe/MFI catalyst with a similar iron load, but containing mostly Fe<sub>2</sub>O<sub>3</sub> particles, was synthesized by incipient wetness impregnation of H/MFI with a concentrated aqueous solution of Fe(NO<sub>3</sub>)<sub>3</sub>, followed by drying and calcination at 550°C.

## 2.2. H<sub>2</sub>-Temperature-Programmed Reduction (TPR)

Before each H<sub>2</sub>-TPR run, the catalyst was calcined in O<sub>2</sub> at 500°C for 60 min. H<sub>2</sub>-TPR was performed with an H<sub>2</sub>/Ar (5%) flow of 40 ml/min by heating the catalyst from 25°C with a ramp of 8°C/min and holding it at the desired final temperature for 60 min. After each H<sub>2</sub>-TPR run, the catalyst was cooled, usually to 250°C, for the N<sub>2</sub>O treatment. Then <sup>18</sup>O<sub>2</sub> isotopic exchange or another H<sub>2</sub>-TPR was performed.

## 2.3. N<sub>2</sub>O Treatment and <sup>18</sup>O<sub>2</sub> Isotopic Exchange

Treatment of Fe/MFI with N<sub>2</sub>O at 250°C was performed in a recirculating manifold equipped with a Dycor quadrupole gas analyzer, and 0.2 g Fe/MFI was charged in a U-shaped Pyrex reactor with a bypass valve. The volume of the circulation loop was 145 ml when the reactor was bypassed, but 166 ml when it was part of the loop. An electromagnet-driven gas-circulation pump was installed inside the loop to enforce gas circulation through the catalyst bed with a flow rate of 100 ml/min. Pressure was monitored by a TC gauge in the range of 0.1–200 Torr and an ionization gauge in the 10<sup>-6</sup> to 10<sup>-2</sup> Torr range. A mixture of 30 Torr N<sub>2</sub>O, 20 Torr Ar, and 70 Torr He was used for the N<sub>2</sub>O treatment. The <sup>18</sup>O<sub>2</sub> exchange reaction was carried out at 250°C by circulating a mixture of 20 Torr <sup>18</sup>O<sub>2</sub>, 20 Torr Ar, and 80 Torr He. All mass spectrometric signal intensities were normalized with respect to the AR<sup>2+</sup> peak (*m/e* = 20). The kinetic data were evaluated as described previously (5, 15). Here we briefly introduce the evaluation procedure.

The following definitions are used: *N<sub>g</sub>*, number of oxygen atoms in the gas phase; *N<sub>s</sub>*, number of exchangeable oxygen atoms in the solid phase (also called pool size);  $\alpha = (^{18}\text{O}_2 + ^{18}\text{O}^{16}\text{O}/2)/(^{18}\text{O}_2 + ^{18}\text{O}^{16}\text{O} + ^{16}\text{O}_2)$ , the fraction of <sup>18</sup>O in the gas-phase oxygen;  $\alpha_0$  and  $\alpha_t$  are the values of  $\alpha$  at *t* = 0 and *t* = *t*, respectively;  $\alpha_\infty$  is the value of  $\alpha$  at the end of a run, when the slope of oxygen isotope concentration with respect to time is 0; and *k*, rate constant for isotopic exchange.

From the material balance it follows that

$$\alpha_0(N_g) = \alpha_\infty(N_g + N_s);$$

therefore,

$$N_s = N_g[\alpha_0/\alpha_\infty - 1]$$

The rate constant *k* is calculated from the first-order plot

$$\ln \left[ \frac{(\alpha_t - \alpha_\infty)}{(\alpha_0 - \alpha_\infty)} \right] = -kt.$$

If the latter graph shows a clear break, more than one pool of oxygen exists in the solid. In that case the pool sizes *N<sub>s1</sub>*, *N<sub>s2</sub>*, . . . are calculated by assuming that the most active pool reaches equilibrium with the gas phase while exchange with the less active pools is negligible. With this assumption one can write, for the most active pool,

$$\alpha_0(N_g) = \alpha_{\text{break}}(N_g + N_{s1})$$

If that assumption is not strictly valid and some <sup>18</sup>O leaks from the most active to the less active pool(s), the calculated value of *N<sub>s1</sub>* will be higher than the true value.

## 3. RESULTS

After calcination in O<sub>2</sub> of 1 bar at 500°C, the <sup>18</sup>O<sub>2</sub> exchange activity of Fe/MFI at 250°C was negligible, irrespective of the preparation method, either sublimation or incipient wetness impregnation. This shows that neither the bridging oxygen atoms of the Fe dimers in MFI nor those in Fe<sub>2</sub>O<sub>3</sub> clusters are exchangeable with <sup>18</sup>O<sub>2</sub> at 250°C. Likewise, N<sub>2</sub>O does not decompose or dissociate on Fe/MFI that was merely calcined at 500°C. Exchange at 250°C did, however, take place with Fe/MFI after one of the following three treatments.

### 3.1. Reduction at 600°C Followed by Exposure to N<sub>2</sub>O at 250°C

In Fig. 2 of our previous work (12) we reported N<sub>2</sub>O dissociation at 250°C on Fe/MFI that was prereduced by H<sub>2</sub>-TPR at 600°C. We found that N<sub>2</sub>O (*m/e* = 44) is readily consumed and N<sub>2</sub> is produced. Reaction appeared to be complete at about 250 min. No gas-phase O<sub>2</sub> could be detected; i.e., the number of O atoms deposited on the surface was equal to the number of N<sub>2</sub> molecules that appeared in the gas phase. The ratios N<sub>2</sub>/Fe and O<sub>dep</sub>/Fe are equal to 0.7. If this state is followed by an H<sub>2</sub>-TPR run, consumption of H<sub>2</sub> is observed as a sharp spike at 200°C.

If exposure to N<sub>2</sub>O is followed by an <sup>18</sup>O<sub>2</sub> isotopic exchange test at 250°C, instead of an H<sub>2</sub>-TPR run, exchange is rapid as shown in Fig. 1a. Clearly, the main exchange product is <sup>18</sup>O<sup>16</sup>O, showing that the R<sup>1</sup> mechanism is dominant. A first-order plot is shown in Fig. 2a, where the logarithm of  $[(\alpha_t - \alpha_\infty)/(\alpha_0 - \alpha_\infty)]$  is plotted versus reaction time. Clearly, this plot shows two linear segments separated by a sharp break, indicating that two pools of exchangeable oxygen exist. The rate constants are calculated from the slopes of the linear parts and listed in Table 1. The pool

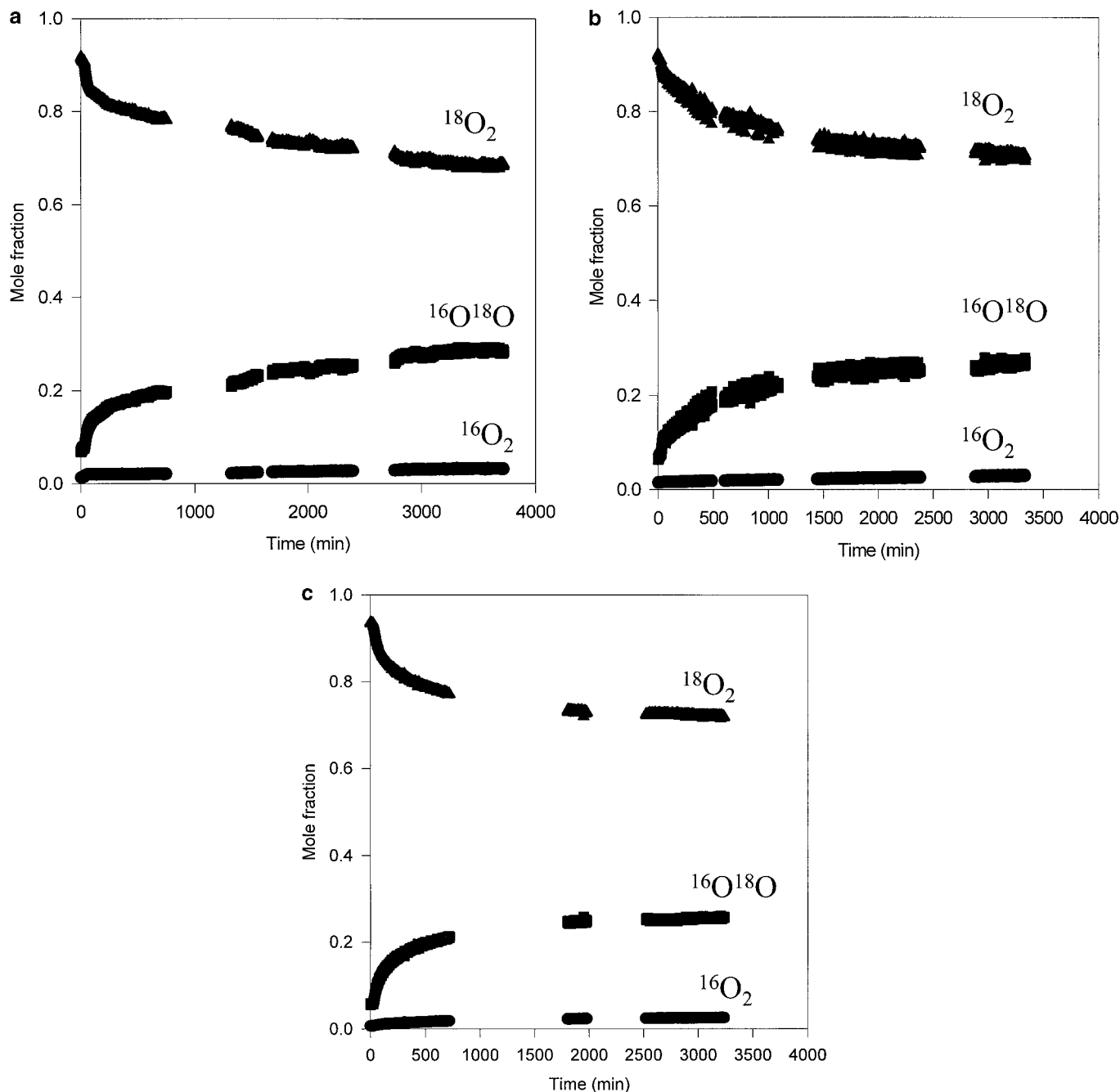


FIG. 1.  $^{18}\text{O}_2$  isotopic exchange at  $250^\circ\text{C}$  with Fe/MFI activated by  $\text{N}_2\text{O}$  at  $250^\circ\text{C}$  after different pretreatments: (a) reduction at  $600^\circ\text{C}$ , (b) reduction at  $500^\circ\text{C}$  followed by evacuation at  $700^\circ\text{C}$ , and (c) reduction at  $700^\circ\text{C}$ .

sizes of exchangeable oxygen in Fe/MFI were calculated and are summarized in Table 2. It follows that about half of the oxygen atoms that were deposited on the catalyst by dissociating  $\text{N}_2\text{O}$  molecules are exchangeable at  $250^\circ\text{C}$ .

### 3.2. Reduction at $500^\circ\text{C}$ , Followed by Evacuation at $700^\circ\text{C}$ , Followed by Exposure to $\text{N}_2\text{O}$ at $250^\circ\text{C}$

$\text{N}_2\text{O}$  dissociations at  $250^\circ\text{C}$  on Fe/MFI that was pre-reduced at  $500^\circ\text{C}$  are similar to those in Fig. 2 of our previous

work (12), but the ratio  $\text{N}_2/\text{Fe}$  is equal to 0.5 (not shown). However, with this material no oxygen isotopic exchange was detectable at  $250^\circ\text{C}$ .

$\text{N}_2\text{O}$  dissociations at  $250^\circ\text{C}$  on another Fe/MFI sample that was also pre-reduced at  $500^\circ\text{C}$ , but was subsequently evacuated at  $700^\circ\text{C}$ , are similar to those in Fig. 2 of our previous work, too (12) (not shown). Again,  $\text{N}_2$  is the only gas-phase product, and in this case the ratio  $\text{N}_2/\text{Fe}$  is equal to 0.7. Because it is not expected that thermal reduction at  $700^\circ\text{C}$  is more intense than chemical reduction with  $\text{H}_2$

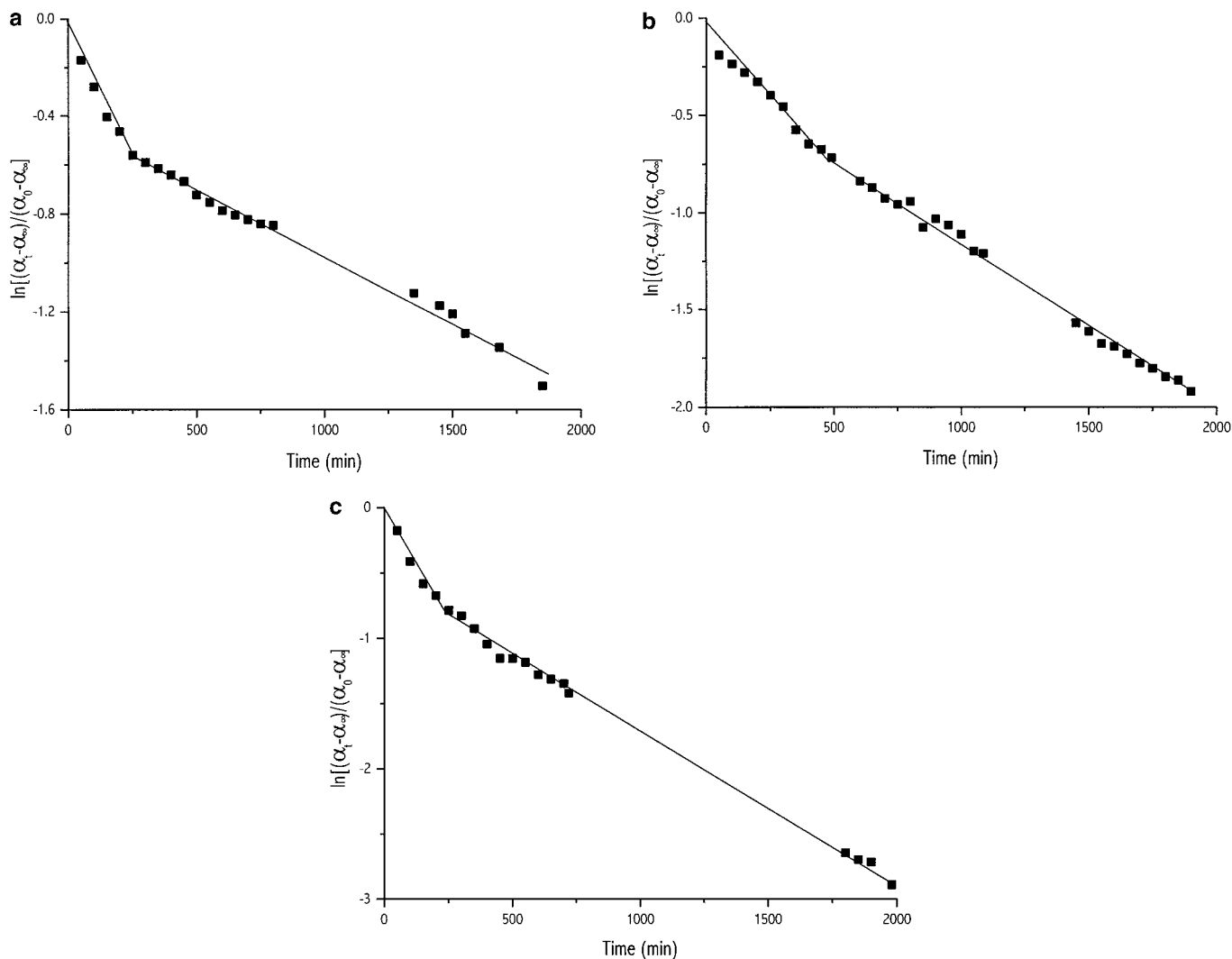


FIG. 2. The kinetics of the  $^{18}\text{O}_2$  isotopic exchange at  $250^\circ\text{C}$  with Fe/MFI activated by  $\text{N}_2\text{O}$  at  $250^\circ\text{C}$  after different pretreatments: (a) reduction at  $600^\circ\text{C}$ , (b) reduction at  $500^\circ\text{C}$  followed by evacuation at  $700^\circ\text{C}$ , and (c) reduction at  $700^\circ\text{C}$ .

at  $500^\circ\text{C}$ , it follows that evacuation at  $700^\circ\text{C}$  changes the state of the solid in a different way. Desorption of water, resulting in coordinative unsaturation of the Fe ions, probably is responsible for the different response of the solid to exposure to  $\text{N}_2\text{O}$ .

TABLE 1

Rate Constants of  $^{18}\text{O}_2$  Isotopic Exchange at  $250^\circ\text{C}$  with Fe/MFI Treated under Different Conditions

Treatment	$k_1$ ( $\text{min}^{-1}$ )	$k_2$ ( $\text{min}^{-1}$ )
$\text{H}_2$ red'n @ $600^\circ\text{C}$ $\text{N}_2\text{O}$ re-ox'n @ $250^\circ\text{C}$	$2.1 \times 10^{-3}$	$5.5 \times 10^{-4}$
$\text{H}_2$ red'n @ $700^\circ\text{C}$ $\text{N}_2\text{O}$ re-ox'n @ $250^\circ\text{C}$	$3.1 \times 10^{-3}$	$1.2 \times 10^{-3}$
$\text{H}_2$ red'n @ $500^\circ\text{C}$ Evacuation @ $700^\circ\text{C}$ $\text{N}_2\text{O}$ Re-ox'n @ $250^\circ\text{C}$	$1.5 \times 10^{-3}$	$8.6 \times 10^{-4}$

The  $^{18}\text{O}_2$  isotopic exchange at  $250^\circ\text{C}$  with the Fe/MFI catalyst and its kinetics were studied and the results are shown in Figs. 1b and 2b. The  $\text{R}^1$  mechanism is still dominant. The rate constants and the pool sizes of exchangeable oxygen are compiled in Tables 1 and 2, respectively. Pretreatment at high temperature thus is a prerequisite for the formation of rapidly exchangeable oxygen from  $\text{N}_2\text{O}$ .

### 3.3. Reduction at $700^\circ\text{C}$ , Followed by Exposure to $\text{N}_2\text{O}$ at $250^\circ\text{C}$

Figure 3 shows  $\text{N}_2\text{O}$  dissociation at  $250^\circ\text{C}$  on Fe/MFI that was prerduced at  $700^\circ\text{C}$ . At this temperature, part of the Fe ions is reduced to  $\text{Fe}^0$  (not shown).  $\text{N}_2$  is the only gas-phase product; the ratio  $\text{N}_2/\text{Fe}$  is equal to 1.3. Part of the consumed oxygen is used to oxidize  $\text{Fe}^0$ . The result of a subsequent  $^{18}\text{O}_2$  exchange run at  $250^\circ\text{C}$  and its kinetics are shown in Figs. 1c and 2c. Again, the  $\text{R}^1$  mechanism is dominant. The

TABLE 2  
Pool Sizes of Exchangeable Oxygen in Fe/MFI Treated in Different Conditions

Treatment	Pool size ( $10^{20}$ sites/g)	Pool size of strong subpool ( $10^{20}$ sites/g)	Pool size of weak subpool ( $10^{20}$ sites/g)	Exchangeable O/Fe (from oxygen exchange)	O number integrated from H <sub>2</sub> -TPR spike at 200°C ( $10^{20}$ sites/g)
H <sub>2</sub> red'n @ 500°C N <sub>2</sub> O re-ox'n @ 250°C	0	0	0	0	0
H <sub>2</sub> red'n @ 600°C N <sub>2</sub> O re-ox'n @ 250°C	1.3	0.6	0.7	0.32	1.1
H <sub>2</sub> red'n @ 500°C Evacuation @ 700°C N <sub>2</sub> O re-ox'n @ 250°C	1.1	0.6	0.5	0.27	1.0
H <sub>2</sub> Red'n @ 700°C N <sub>2</sub> O Re-ox'n @ 250°C	1.2	0.6	0.6	0.30	1.0

rate constants and the pool sizes of exchangeable oxygen in Fe/MFI are summarized in Tables 1 and 2, respectively. Remarkably, the pool sizes, derived from the exchange data, are almost constant while the  $O_{\text{dep}}/\text{Fe}$  ratios vary between 0.7 and 1.3. This indicates that the isotopic exchange specifically detects the active oxygen ligated to coordinatively unsaturated Fe ions, whereas the  $O_{\text{dep}}/\text{Fe}$  ratio also includes oxygen from N<sub>2</sub>O that is bridging over two Fe<sup>2+</sup> ions or converts Fe<sup>0</sup> to oxide clusters. The number of exchangeable O atoms is, however, equal within experimental error to the number counted by integrating the sharp H<sub>2</sub>-TPR spike at 200°C (see Table 2).

### 3.4. Reduction at 500°C, Followed by Evacuation at 700°C, Followed by Exposure to H<sub>2</sub>O Vapor at 25°C, Followed by Exposure to N<sub>2</sub>O at 250°C

After reduction at 500°C, followed by evacuation at 700°C, the Fe/MFI was exposed for 10 min to an H<sub>2</sub>O/Ar flow with a flow rate of 100 ml/min at 25°C. The N<sub>2</sub>O decomposition at 250°C on Fe/MFI results are similar to those in Fig. 2 of our previous work (12) but N<sub>2</sub>/Fe = 0.5. Subsequently, the solid was exposed to <sup>18</sup>O<sub>2</sub> at 250°C. Exchange was found to be negligible. It is remarkable that adsorption of water has only a minor effect on the dissociation of N<sub>2</sub>O at 250°C, but its effect on the exchangeability of the deposited oxygen against gas-phase <sup>18</sup>O<sub>2</sub> is quite dramatic.

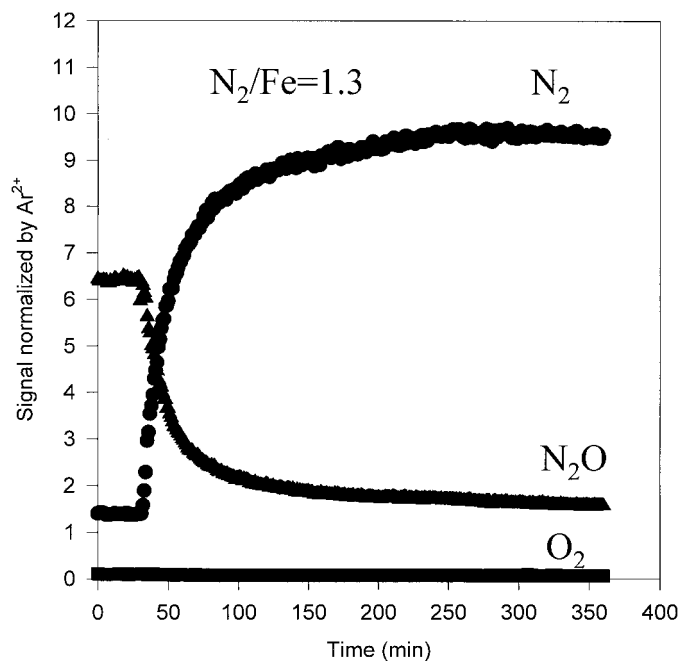


FIG. 3. Dissociative adsorption of N<sub>2</sub>O at 250°C on Fe/MFI after reduction at 700°C.

## 4. DISCUSSION

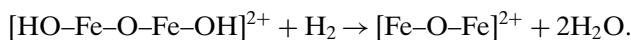
Part of the oxygen deposited on Fe/MFI by dissociating N<sub>2</sub>O is chemically highly active and exchanges with gaseous <sup>18</sup>O<sub>2</sub> at high rate. Our previous results (5) showed that oxygen of Fe oxide clusters in MFI cavities is exchangeable at a higher rate than bridging oxygen of dinuclear oxo ions or any oxygen of the zeolite lattice. In that work, temperatures above 375°C were required to obtain exchange rates that could be monitored with the equipment used here. In contrast, a temperature of 250°C suffices in the present work to obtain a high initial exchange rate, as demonstrated in Fig. 1. This high activity matches the sharp and highly exothermic TPR spike created by the same oxygen. The results leave no doubt that exposure to N<sub>2</sub>O of Fe/MFI that had been pretreated at high temperature creates an unusually active oxygen species that is qualitatively different from the oxide and oxo ion species, described earlier.

A second conclusion from the present results is that the new active oxygen species strictly follow the R<sup>1</sup> mechanism as expected for fairly isolated oxygen atoms. A third conclusion is that the number of O atoms that are exchangeable in

this manner are not identical to the number of O atoms deposited from N<sub>2</sub>O, but usually the former number is smaller, because the latter includes oxygen consumed in reoxidizing any prereduced iron species. An important element of isotopic exchange kinetics is the constancy of the degree of surface coverage when only atoms of one isotope are exchanged against chemically identical atoms of a different isotope. Any heterogeneity observed under such circumstances must be an *a priori* heterogeneity, whereas *induced* heterogeneities become manifest only when the degree of coverage is changed.

While these conclusions are fairly straightforward, additional assumptions are needed to discuss the possible structure of the active oxygen–iron complex. Besides the present experimental data and those of Panov's group, theoretical results should be mentioned, such as the recent study by Yakovlev *et al.* (13). Moreover, the close analogy between the mono- and dinuclear Fe sites on MFI and the sites in enzymes such as cytochrome P-450 and the class of the methane monooxygenase (MMO) enzymes might be relevant (16). When combining this evidence with that reported earlier, a tentative explanation can be proposed for the unexpected finding wherein the first-order plot in Fig. 2 displays a break which appears to indicate that the pool of easily exchangeable oxygen actually consists of two subpools.

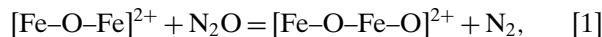
Our interpretation of the current results is based on the evidence that after calcination the present Fe/MFI catalysts contains a significant portion of the Fe ions as Fe<sup>3+</sup> in dinuclear oxygen-bridged ions, such as [HO–Fe–O–Fe–OH]<sup>2+</sup>. The current data show that two conditions must be fulfilled to make this material susceptible to form highly active oxygen by interaction with N<sub>2</sub>O: (1) Fe<sup>3+</sup> is to be reduced to Fe<sup>2+</sup> and (2) a treatment at high temperature is required. We assume that this treatment brings some Fe<sup>2+</sup> ions in a state of high coordinative unsaturation, because readsorption of H<sub>2</sub>O destroys this state. It follows that either isolated Fe<sup>2+</sup> ions are formed or the dinuclear oxo ions, after losing one O<sup>2-</sup> ion and one H<sub>2</sub>O molecule, are transformed to oxygen-bridged dinuclear ions with Fe<sup>2+</sup>:



If an isolated Fe<sup>2+</sup> reacts with an N<sub>2</sub>O molecule, a ferryl group [Fe=O]<sup>2+</sup> will be formed. Its reduction with H<sub>2</sub> or CO or its interaction with another N<sub>2</sub>O molecule should regenerate the Fe<sup>2+</sup> ion, while H<sub>2</sub>O, CO<sub>2</sub>, or N<sub>2</sub> + O<sub>2</sub> is formed. The latter possibility is excluded under the conditions used here, since no O<sub>2</sub> was released.

For the key intermediate **Q** of MMO with an Fe<sup>4+</sup>–O distance of 1.77 Å, Shu *et al.* (17) reported an “Fe<sub>2</sub><sup>IV</sup>O<sub>2</sub> diamond” core structure. This value is in good agreement with the Fe–O distance of 1.81 Å for Fe/MFI exposed to N<sub>2</sub>O and attributed to [Fe<sup>4+</sup>O]<sup>2+</sup> (12).

Formation of [Fe–O–Fe]<sup>2+</sup> was considered by Yakovlev *et al.* (13). They conclude from their DFT analysis that interaction of N<sub>2</sub>O with this ion transforms it into an [Fe–O–Fe–O]<sup>2+</sup> ion with a terminal Fe<sup>4+</sup>–O<sup>-</sup> bond, while N<sub>2</sub> is released. For the terminal Fe–O group, their calculations predict an Fe–O distance of 1.61 Å, indicating double-bond character. For the reaction

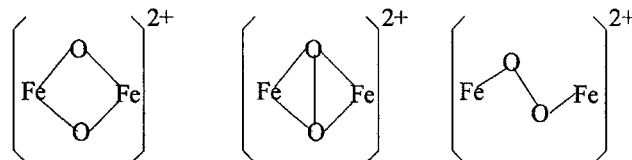


a standard reaction enthalpy of ΔH<sub>1</sub> = –132 kJ/mol is calculated. From this value it follows that for subsequent reduction with H<sub>2</sub>,



should be exothermic by 192 kJ/mol. This high exothermicity is in line with the observed sharp H<sub>2</sub>-TPR spike. Much lower values are calculated by Arbuznikov and Zhidomirov for the interaction of N<sub>2</sub>O with hydrated Fe dimers (18).

For the four-atom ion [Fe–O–Fe–O]<sup>2+</sup>, several isomers were discussed for μ-oxo Fe dimer compounds (19, 20) including the following:



We believe that this family of [Fe<sub>2</sub>O<sub>2</sub>]<sup>2+</sup> ions should be considered in addition to the mononuclear [Fe=O]<sup>2+</sup> ion as potential candidates for the product of dissociative N<sub>2</sub>O adsorption on iron ions in partially prereduced and dehydrated Fe/MFI.

#### ACKNOWLEDGMENT

This work was supported by the EMSI program of the National Science Foundation and the U.S. Department of Energy, Office of Science (CHE-9810378) at the Northwestern University Institute for Environmental Catalysis. Support from the Director of the Chemistry Division, BES, U.S. Department of Energy, Grant DE-FGO2-87ER13654, is gratefully acknowledged.

#### REFERENCES

1. Winter, E. R. S., *J. Chem. Soc. A* **12**, 2889 (1968).
2. Boreskov, G. K., *Adv. Catal.* **15**, 285 (1964).
3. Klier, K., Novakova, J., and Jiru, P., *J. Catal.* **2**, 479 (1963).
4. Panov, G. I., *CatTech* **7**, 18 (2000).
5. Voskoboinikov, T. V., Chen, H. Y., and Sachtler, W. M. H., *J. Mol. Catal. A* **155**, 155 (2000).
6. Doornkamp, C., Clement, M., and Ponc, V., *J. Catal.* **182**, 300 (1999).
7. Chen, H. Y., and Sachtler, W. M. H., *Catal. Today* **42**, 73 (1998).
8. Sun, Q., Gao, Z., Chen, H. Y., and Sachtler, W. M. H., *J. Catal.* **201**, 89 (2001).
9. Marturano, P., Drozdová, L., Kogelbauer, A., and Prins, R., *J. Catal.* **192**, 236 (2000).

10. Battiston, A. A., Bitter, J. H., and Koningsberger, D. C., *Catal. Lett.* **66**, 75 (2000).
11. El Malki, El M., van Santen, R. A., and Sachtler, W. M. H., *Micro-porous Mater.* **35**, 235 (2000).
12. Jia, J., Sun, Q., Wen, B., Chen, L. X., and Sachtler, W. M. H., *Catal. Lett.* in press.
13. Yakovlev, A. L., Zhidomirov, G. M., and van Santen, R. A., *J. Phys. Chem. B* **105**, 12297 (2001).
14. Mauvezin, M., Delahay, G., Coq, B., Kieger, S., Jumas, J. C., and Olivier-Fourcade, J., *J. Phys. Chem. B* **105**, 928 (2001).
15. Tsuchiya, S., Ponec, V., and Sachtler, W. M. H., *J. Catal.* **22**, 280 (1971).
16. Merckx, M., Kopp, D. A., Sazinsky, M. H., Blazyk, J. L., Muller, J., and Lippard, S. J., *Angew. Chem., Int. Ed. Engl.* **40**, 2782 (2001).
17. Shu, L., Nesheim, J. C., Kauffmann, K., Munck, E., Lipscomb, J. D., and Que, L., Jr., *Science* **275**, 515 (1997).
18. Arbuznikov, A. V., and Zhidomirov, G. M., *Catal. Lett.* **40**, 17 (1996).
19. Solomon, E. I., Brunold, T. C., Davis, M. I., Kemsley, J. N., Lee, S. K., Lehnert, N., Neese, F., Skulan, A. J., Yang, Y. S., and Zhou, J., *Chem. Rev.* **100**, 235 (2000).
20. Siegbahn, P. E. M., and Crabtree, R. H., *J. Am. Chem. Soc.* **119**, 3103 (1997).